Efficient removal U(VI) from simulated seawater with hyperbranched polyethylenimine (HPEI) covalently modified SiO_2 coated magnetic microspheres

Wenting Li[a,b], Qi Liu[a,b], Rongrong Chen[a,c], Jing Yu[a,b], Hongsen Zhang[a], Jingyuan Liu[a], Rumin Li[a,b,d], Milin Zhang[a,e], Peili Liu[c] and Jun Wang[a, b,c]**

[a.] *Key Laboratory of Superlight Material and Surface Technology, Ministry of Education, Harbin Engineering University, 150001, P. R. China. E-mail: lrm1888@hotmail.com; Fax: +86 451 8253 3026; Tel: +86 451 8253 3026; E-mail address: zhqw1888@sohu.com*

[b.] *College of Materials Science and Chemical Engineering, Harbin Engineering University, 150001,P. R. China.*

[c.] *Institute of Advanced Marine Materials, Harbin Engineering University, 150001, P. R. China.*

[d.] *Harbin Engineering University Assets Management Co., LTD, 150001, P. R. China.*

[e.] *College of science, Heihe University, 164300, PR China.*

Characterization method

Fourier-transform infrared (FT-IR) spectra were recorded with an AVATAR 360 FT-IR spectrophotometer with the samples pressed into standard KBr pellets. The morphological properties of PAN-HPEI were investigated by using a scanning electron microscope (SEM) equipped with an energy dispersive X-ray spectrometry analyzer (EDS, INC250, Japan Electronic). X-ray photoelectron spectroscopy (XPS) measurements were performed by a Thermo ESCALAB 250Xi spectrometer with monochromated Al Kα radiation (hν= 1846.6 eV). The binding energy scale of spectrometer was calibrated using the metallic Cu $2p_{3/2}$ lines and Ag Fermi Edge of the respective reference metals. The binding energy of C 1s (284.6 eV) was used as a reference to eliminate charge effects. The zeta potential was determined by a Malvern Instrument ZetaSizer Nano ZS90.

The concentration of U(VI) at mg L^{-1} or μg L^{-1} level was determined using Inductively Coupled Plasma-Atomic Emission Spectroscopy (**ICP-AES**) with an IRIS Intrepid II XSP instrument, or using Inductively Coupled Plasma-Mass Spectrometry (**ICP-MS**) with a X Series^{II} instrument. All experiments mentioned above were carried out in triplicate tests, and the reported results were average values of three data sets.

Batch Equilibrium U(VI) Adsorption Experiments.

Batch Equilibrium U(VI) Adsorption Experiments were cconducted in a battery of conical flasks (100 mL) in which a specified dosage of the adsorbent was shaken with U(VI) solution (50 mL) of assigned concentration and pH in a thermostatic water shaker at a speed of 150 rpm. The initial pH of the solution was regulated with negligible volumes of 0.5 M NaOH or HNO_3 solution. The mixture was shaken in a

thermostatic shaker bath. After the magnetic microspheres separated by an applied magnet, the concentration of U(VI) in the solution was measured for further calculation.

The adsorption experiments in simulated seawater were also conducted to get a relatively reasonable result for the expected results in actual marine conditions for 48 h. The simulated seawater was prepared according to our earliest work.[19] By dissolving 2.11 g uranyl nitrate and 33 g sea salt in 1 L DI water, the artificial seawater with the concentration of 1000 mg L^{-1} was synthesized. Afterwards, the as-prepared seawater was diluted to μg L^{-1} level ranging from 3 to 30 μg L^{-1} to mimic seawater environment.

Adsorption Kinetics:

Assuming that the adsorption is controlled by diffusion step, the pseudo-first order equation is written as:

$$\ln\left(Q_e - Q_t\right) = \ln Q_e - k_1 t \qquad \text{(S1)}$$

Where k_1 is the rate constant of pseudo-first order adsorption, Q_e and Q_t (mg g^{-1}) are the amount of U(VI) adsorbed at equilibrium and at time (t), respectively.

And assuming that the adsorption process is controlled by the chemical adsorption, the pseudo-second order equation is given as:[1]

$$t / Q_t = 1 / (k_2 \cdot Q_e^{\,2}) + t / Q_e \qquad \text{(S2)}$$

Where k_2 is the rate constant of pseudo-second order equation.

To further catch on the rate controlling steps, intra-particular diffusion model in view of the assumption that liquid film diffusion resistance is negligibly small was applied to study the adsorption process, and the equation based upon Weber-Morris equation was described as follows:

$$Q_t = k_3 t^{0.5} + C \qquad \text{(S3)}$$

Where k_3 (mg g^{-1} $min^{-0.5}$) is the intra-particular diffusion rate constant and C (mg g^{-1}) is a constant proportional to the boundary layer, respectively. The higher value of C is, the greater contribution of the boundary layer makes.

[1] S.W. Zhang, M.Y. Zeng, J.X. Li, J. Li, J.Z. Xu, X.K. Wang, Porous magnetic carbon sheets from biomass as an adsorbent for the fast removal of organic pollutants from aqueous solution, J. Mater. Chem. A 2 (2014) 4391–4397.

[2] Y.-S. Ho, G. McKay, The kinetics of sorption of divalent metal ions onto sphagnum moss peat, Water Res. 34 (2000) 735–742.

[3] T. Wen, Q. Fan, X. Tan, Y. Chen, C. Chen, A. Xu, X. Wang, A core–shell structure of polyaniline coated protonic titanate nanobelt composites for both Cr(VI) and humic acid removal, Polym. Chem. 7 (2016) 785–794.

Adsorption isotherms:

The Langmuir isotherm, as one of the most famous well-adopted models used to describe the adsorption systems from solutions, has been utilized extensively for dilute solutions in the following equation:[2]

$$Q_e = b \cdot q_m \cdot C_e / (1 + bC_e) \qquad \text{(S4)}$$

Where Q_m (mg g^{-1}) is the maximum adsorption capacity, b is the Langmuir adsorption

equilibrium constant.

The separation factor constant (R_L) is a factor revealing the applicability of the fiber towards a targeted metal ion and may be calculated from the equation:

$$R_L = \frac{1}{1+bC_0} \qquad \text{(S5)}$$

The value of R_L provides guidance for the possibility of the adsorption process to proceed. $R_L > 1.0$, unsuitable; $R_L = 1.0$, linear; $0 < R_L = 1.0$, suitable; $R_L = 0$, irreversible. The values of R_L, as displayed in **Fig. 7B**, were found to range from 0.00587 to 0.19333, indicating the suitability of PAN-HPEI as adsorbents for the recovery of U(VI) ions from aqueous solutions.

Another factor can help understanding the behavior of the adsorption of U(VI) ions on PAN-HPEI, is the Langmuir surface coverage rate (θ), which relates the surface coverage of the fiber to the initial concentration of U(VI) ions and can be calculated using the following equation:[3]

$$\theta = \frac{bC_0}{1+bC_0} \qquad \text{(S6)}$$

The relationship of θ and initial concentration of U(VI) ions was depicted in **Fig. 7C**. Evidently, the adsorption of U(VI) ions on PAN-HPEI in the early age was very fast (low coverage of fiber surface and plenty of free active sites are available for binding with the metal ions) then tends to be a plateau at higher surface coverage where most of the active sites are occupied. This implies the applicability of Langmuir model to describe the adsorption of U(VI) ions on PAN-HPEI.

The Freundlich model is based on a reversible heterogeneous adsorption since it is not restricted to monolayer adsorption capacity [36]. The Freundlich isotherm equation is given as:

$$Q_e = K_f \cdot C_e^{1/n} \qquad \text{(S7)}$$

Where k and n are the Freundlich constants related to the adsorption capacity and adsorption intensity, respectively.

The Sips model is according to the combination of Langmuir and Freundlich model, and the mathematical formula is as follows:

$$Q_e = \frac{Q_s K_s C_e^m}{1+K_s C_e^m} \qquad \text{(S8)}$$

Where Q_s is the saturated adsorption capacity, K_s is the Sips constant related to the adsorption energy and m is the Sips constant. When the 1/m equals to zero the adsorption is heterogeneous adsorption, while the homogeneous adsorption happens when 1/m is 1.

The D-R model, which is applied to get further information of the nature of the adsorption process [41], is on the basis of assumption that a Gaussian energy distribution onto a heterogeneous surface with an expression of the following equations:

$$Q_e = Q_{DR} e^{(-\beta\varepsilon^2)} \qquad \text{(S9)}$$

$$\varepsilon = RT \ln(1+\frac{1}{C_e}) \qquad \text{(S10)}$$

$$E = 1/\sqrt{2\beta} \qquad \text{(S11)}$$

Where Q_{DR} (mg g^{-1}) is the monolayer saturated adsorption capacity, β (mol^2 kJ^{-2}) is related to the free energy of adsorption and E (kJ mol^{-1}) stands for the mean free energy which can be used as the indicator whether the process is manipulated by physical adsorption.

Entropy ($\Delta S°$) and enthalpy ($\Delta H°$) changes were calculated using the following equation:[4]

$$\ln K_D = -\Delta H° / RT + \Delta S° / R \qquad \text{(S12)}$$

Where K_D is the equilibrium constant (mL g^{-1}), $\Delta H°$ is standard enthalpy (kJ mol^{-1}), $\Delta S°$ is standard entropy (J mol^{-1} K^{-1}), T is the absolute temperature (K), and R is the gas constant (8.314 J mol^{-1} K^{-1}).

Gibbs free energy (ΔG°), is calculated from the following Gibbs–Helmholtz equation:

$$\Delta G° = \Delta H° - T \cdot \Delta S° \qquad \text{(S13)}$$

Where ΔG° is the standard Gibbs free energy.

[4] G. Moussavi, R. Khosravi, The removal of cationic dyes from aqueous solutions by adsorption onto pistachio hull waste, Chem. Eng. Res. Des., 89 (2011) 2182-2189.

The Fig. 1D exhibits the N_2 adsorption−desorption isotherms and the relevant pore-size distribution curve for the microspheres. The core−shell microspheres exhibit a typical IV isotherm with a remarkable hysteresis loop (P/P_0> 0.45), displaying the presence of mesopores. The result goes a step further by the well-developed mesopores with a diameter of 18.92 nm, which is determined by Barret Joyner Halenda (BJH) method, as shown in the inset. What's more, the specific surface area of the core−shell Fe_3O_4@SiO_2-HPEI microspheres is calculated to be 57.925 m^2 g^{-1} by the Brunauer Emmett Teller (BET) method.

The values of $\Delta S°$ and $\Delta H°$ are assessed from the slope and intercept of the linear plot of ln K_D vs. *1/T* (**Fig. S1**). The positive standard entropy ($\Delta S°$) implies that randomness increases at the solid/solution interface during adsorption. The positive value of $\Delta H°$ exhibits that the extraction process of UO_2^{2+} is endothermic.
From **Eq. (S13)**, the $\Delta G°$ at different temperatures is acquired. The data of $\Delta G°$, $\Delta H°$ and $\Delta S°$ are displayed in **Table S3** in the ESI†**.** The negative values of ΔG° illustrate that the extraction complies with a feasible and spontaneous trend. Gibbs free energy decreases with increase in temperature, which suggests that higher temperatures facilitate adsorption of U(VI) ions onto Fe_3O_4@SiO_2-HPEI due to a greater driving force.

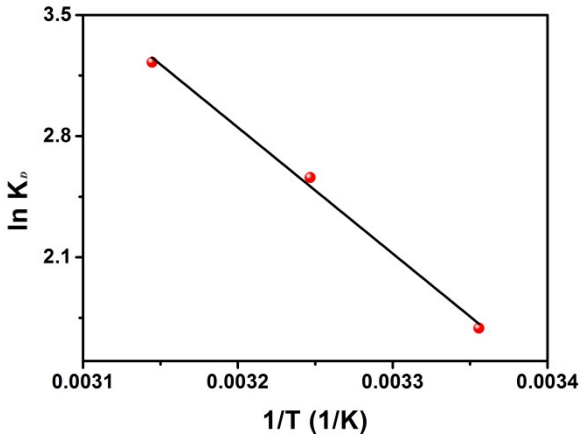

Fig. S1. Van 't Hoff plot for removal of U(VI) by Fe_3O_4@SiO_2-HPEI.

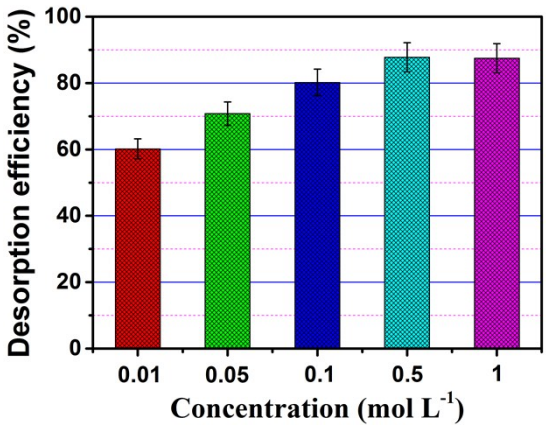

Fig. S4. shows the experimental data of desorption with HCl of different concentration.

Table S1. Kinetic parameters for adsorption of U(VI) on Fe_3O_4@SiO_2-HPEI.

Kinetic model	T (°C)	C_0 (mg/L)	Q_e^{cal} (mg/g)	k_1(min^{-1})/k_2 (g/mg·min)	R^2
Pseudo-first order	25	150	14.68	0.2363	0.9620
Pseudo-second order	25	150	349.65	0.000039	0.9831
Intra-particle diffusion	25	150	261.7	2.61185/ 0.84106/ 0.04787	0.9864

Table S2. Isotherm parameters for adsorption of U(VI) on Fe_3O_4@SiO_2-HPEI

Isotherm parameters	298 K	308 K	318 K
Langmuir isotherm			
q_m(mg U/g)	327.90	344.30	375.08
K_L(L/mg)	0.4218	0.2523	0.1705
R^2	0.8964	0.9148	0.9183
Freundlich isotherm			
K_F(L/g)	64.89	101.70	68.03
n	0.3515	0.3022	0.3874
R^2	0.8299	0.9063	0.9289
Dubinin-Radushkevich (D-R)			
β	1.54×10^{-6}	3.62×10^{-7}	9.03×10^{-8}
Q_{DR}	217.85	211.61	195.05
E	569.85	1174.96	2352.49
R^2	0.8675	0.7406	0.7196
Langmuir-Freundlich (Sips)			
Q_s	280.67	368.94	457.71
K_s	0.0728	0.1912	0.2746
m	0.4104	0.1182	0.5105
R^2	0.9651	0.9817	0.9873

Table S3. Thermodynamic parameters for adsorption of U(VI) on Fe_3O_4@SiO_2-HPEI.

$\Delta H°$ (kJ mol^{-1})	$\Delta S°$ (J mol^{-1} K^{-1})	$\Delta G°$ (kJ mol^{-1})		
		298K	308K	318K
10.21	40.43	-1.76	-2.24	-2.65

Table S4. The maximum adsorption capacity of different adsorbents for U(VI).

Adsorbents	Adsorption Capacity mg-U/g-adsorbent	Conditions	Ref.
graphene oxide-manganese dioxide	185.2	C_0 = 22.5 – 70 mg L^{-1}, m = 10 mg, V = 20 ml T = 298 K, pH = 3.8	[1]
Fe/Fe_3C@porous carbon sheets	140	C_0 not given, $C_{adsorbent}$ = 0.05 g L^{-1}, T = 298 K, pH=4	[2]
Mesoporous polymer-carbon composites containing amidoxime groups	322.6	C_0 not given, m = 10 mg, V = 50 ml T = 298.15 K, pH = 5.0	[3]
imine-functionalized carbon spheres	113.16	C_0= 1 – 100 mg L^{-1}, m = 50mg, V = 20 ml, T = 298K, pH=4	[4]
Wool-AO@TiO_2	113.12	C_0= 10 – 500 mg L^{-1}, m = 20mg, V = 20 ml, T = 298K, pH=8	[5]

ion-imprinted magnetic chitosan resins	187.26	C_0= 15 – 420 mg L^{-1}, m = 50 mg, V = 50 ml T = 298 K, pH = 5	[6]
HLPC-MnO_2	238.09	C_0 = 30 – 300 mg L^{-1}, m = 10 mg, V = 20 ml T = 298 K, pH = 5	[7]
Fe_3O_4@SiO_2-HPEI	280.67	C_0 = 25 –250 mg L^{-1}, m = 10 mg, V = 20 ml T = 298 K, pH = 7	this study

References

1. N. Pan, L. Li, J. Ding, S. Li, R. Wang, Y. Jin, X. Wang and C. Xia, *J. Hazard. Mater.*, 2016, **309**, 107-115.

2. Wang X, Zhang S, Li J, J Xu, X Wang, Fabrication of Fe/Fe_3C@porous carbon sheets from biomass and their application for simultaneous reduction and adsorption of uranium (VI) from solution[J]. Inorganic Chemistry Frontiers, 2014, **1**(8), 641-648,

3. Zhang Z, Dong Z, Wang X, D Ying, F Niu, X Cao, Y Wang, R Hua, Y Liu, X Wang, Ordered mesoporous polymer–carbon composites containing amidoxime groups for uranium removal from aqueous solutions[J]. Chemical Engineering Journal, 2018, **341**, 208-217.

4. S. P. Dubey, A. D. Dwivedi, M. Sillanpää, Y.-N. Kwon and C. Lee, *RSC Adv.*, 2014, **4**, 46114-46121.

5. Wen J, Li Q, Li H, M Chen, S Hu, H Cheng, Nano TiO_2 imparts amidoximated wool fibers with good antibacterial activity and adsorption capacity for uranium (VI) recovery[J]. Industrial & Engineering Chemistry Research, 2018, **57**, 1826−1833

6. L. Zhou, C. Shang, Z. Liu, G. Huang and A. A. Adesina, *J. Colloid Interf. Sci.*, 2012, **366**, 165-172.

7. J. Zhu, Q. Liu, Z. Li, J. Liu, H. Zhang, R. Li, J. Wang, G.A. Emelchenko, Recovery of uranium (VI) from aqueous solutions using a modified honeycomb-like porous carbon material[J]. Dalton Transactions, 2017, **46**(2), 420-429.